Supplementary Material for

Structural and High-Pressure Properties of Rheniite (ReS₂) and (Re,Mo)S₂

Jordi Ibáñez-Insa[1], Tomasz Woźniak[2], Robert Oliva[3], Catalin Popescu[4], Sergi Hernández[5], Julian López-Vidrier[5]

[1]Geosciences Barcelona (GEO3BCN), CSIC, Lluís Solé i Sabarís s/n, 08028 Barcelona, Catalonia, Spain; jibanez@geo3bcn.csic.es
[2]Department of Semiconductor Materials Engineering, Wrocław University of Science and Technology, Wybrzeże Wyspiańskiego 27, 50-370, Wrocław, Poland
[3]Department of Physics and Materials Science, University of Luxembourg, 41 rue du Brill, L-4422 Belvaux, Luxembourg
[4]CELLS-ALBA Synchrotron Light Facility, 08290 Cerdanyola del Vallès (Barcelona), Catalonia, Spain
[5]Department of Electronic and Biomedical Engineering, University of Barcelona, Martí i Franquès 1, 08028 Barcelona, Catalonia, Spain.
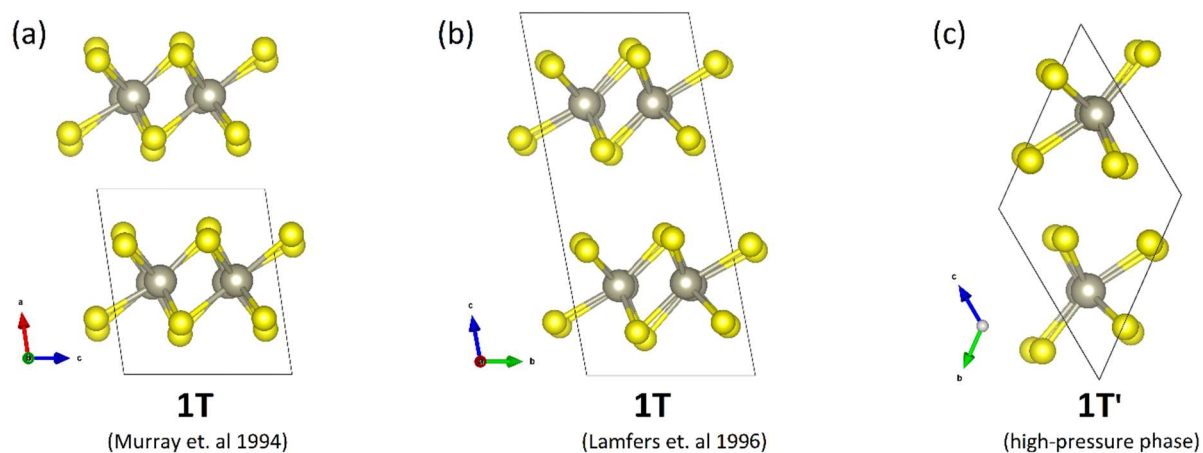
Figure S1. (**a**) Crystal structure of triclinic (distorted CdCl₂ structure, s.g. *P*-1) of ReS₂ at ambient pressure, labeled throughout this work as 1T-ReS₂. This corresponds to the structure published by Murray et al. (Ref. [8] in the manuscript). (**b**) Crystal structure of triclinic (s.g. *P*-1) reported by Lamfers and co-workers (Ref. [9] in the manuscript), where the unit cell is doubled along the direction perpendicular to the ReS₂ sandwiches. (**c**) Crystal structure of the high-pressure ReS₂ phase, labelled throughout this work as 1T'-ReS₂. This phase is denominated as "distorted 1T" in Ref. [19].
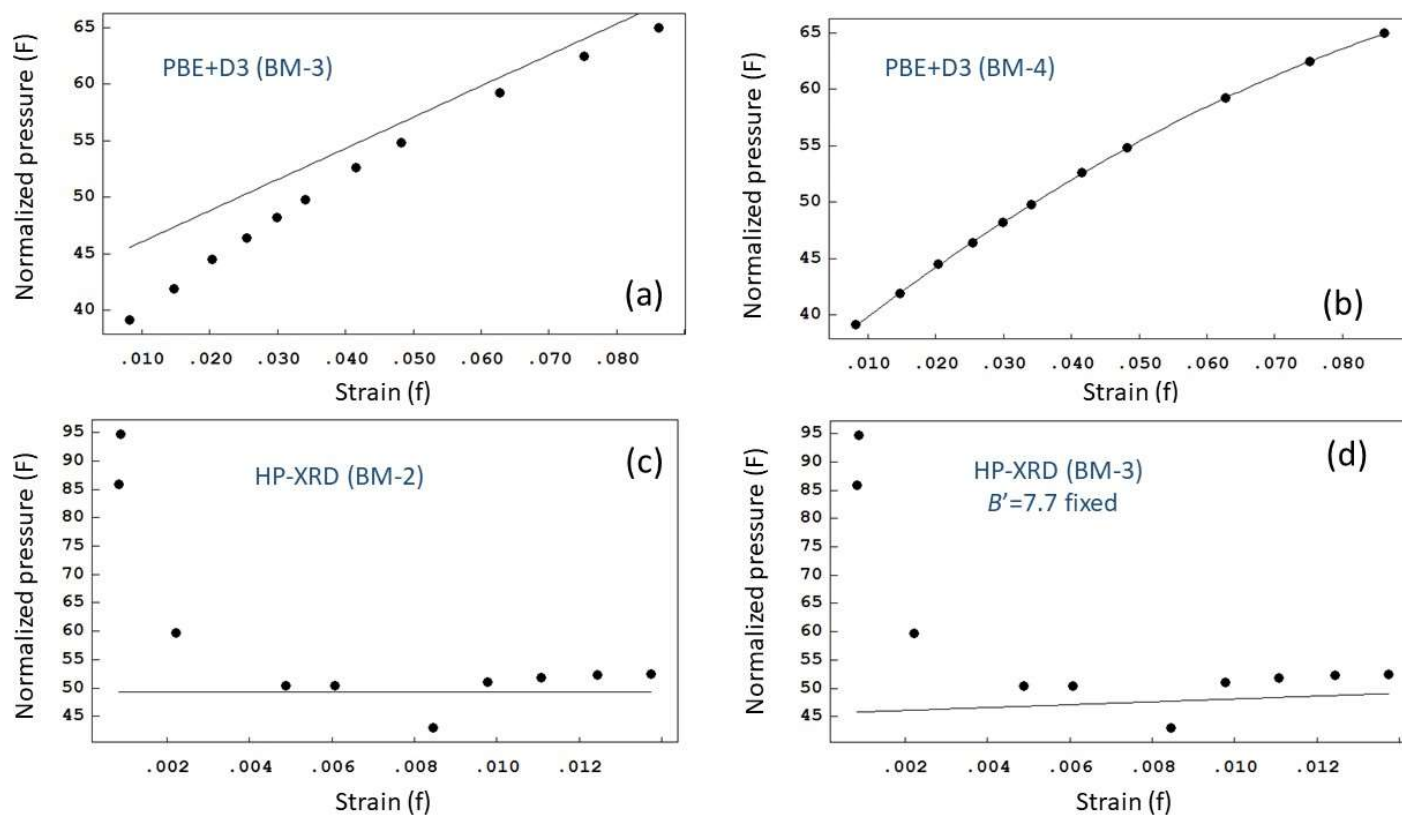
Figure S2. Normalized pressure ($F = P / [3f (2f + 1)^{5/2}]$) vs Eulerian strain ($f = 0.5[(V / V_0)^{-2/3} – 1]$) for different equation of state (EoS) fits performed in this work using 2nd, 3rd or 4th-order Birch–Murnaghan (BM) equations of state [see Angel, R.J., Reviews in Mineralogy and Geochemistry **41**, 35-59 (2000)]. Figures (**a**) and (**b**) show fits to the results of PBE+D3 density functional theory (DFT) calculations up to 25 GPa, using BM-3 and BM-4, respectively. Figures (**c**) and (**d**) show the corresponding F-f plots for the fits to the experimental high-pressure XRD data, using BM-2 and BM-3 (with B' fixed to 7.7), respectively. In all the figures, the dots correspond to calculated (PBE+D3) or experimental (HP-XRD) data points, while the solid lines show the results of the EoS fits. Note that the large variations in F at low f in the case of the experimental data (figures c and d) arise from the large uncertainty in F due to the fact that f tends to zero when V tends to the zero-pressure volume, V_0.
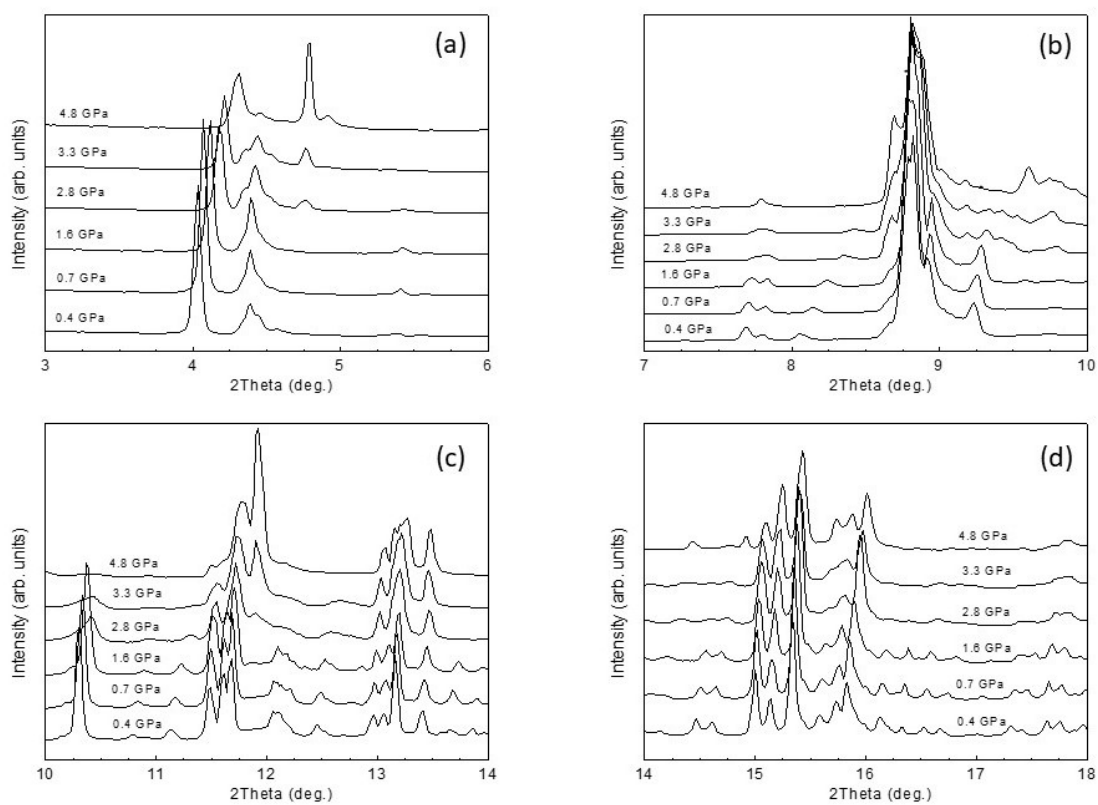
Figure S3. High-pressure synchrotron XRD measurements of synthetic 1T-ReS$_2$ up to ~5 GPa. Figures (**a**) to (**d**) show different angular regions of the scans, which allows highlighting the peak shifts with increasing pressure as well as the appearance of new reflections that can be attributed to the 1T' phase.